Mixed state in magnetic superconductors

M. Tachiki
The Research Institute for Iron, Steel and Other Metals, Tohoku University, Sendai, 980 Japan

H. Matsumoto and H. Umezawa
Department of Physics, University of Alberta, Edmonton, Alberta T6G 2J1, Canada

(Received 23 October 1978)

The boson theory is reformulated in a form applicable to the mixed state in the rare-earth compounds, $R\mathrm{Rh}_4\mathrm{B}_4$, $R_x\mathrm{Mo}_6\mathrm{S}_8$, and $R_x\mathrm{Mo}_6\mathrm{Se}_6$. The magnetic field induced by the persistent current of vortices, and the spin magnetization magnetized by this field are self-consistently calculated. A nonuniform spin magnetization with the periodicity of a flux-line lattice appears in the crystals. The total flux which is the sum of the spin and current contributions is quantized. This quantization effects the current inversion and thus the attractive interaction between the vortices. The calculated magnetization has a tendency of becoming the type-I or type II-1 superconductor even for a large κ. The fact that H_{c2} is drastically depressed near the Curie or Nèel temperature explains the experiments on $\mathrm{Dy}_x\mathrm{Mo}_6\mathrm{S}_8$ and $\mathrm{Er}_x\mathrm{Mo}_6\mathrm{S}_8$.

I. INTRODUCTION

Recently, the rare-earth compounds $R\mathrm{Rh}_4\mathrm{B}_4$, $R_x\mathrm{Mo}_6\mathrm{S}_8$, and $R_x\mathrm{Mo}_6\mathrm{Se}_8$ with $x=1.0$ or 1.2, were found to exhibit superconductivity, although these compounds contain the magnetic moments of rare-earth ions.[1-3] In these compounds, rare-earth ions are placed at the lattice points with regular crystal periodicity. The superconducting and magnetic properties of these compounds show many characteristic features. Some of them are as follows. Superconductivity in $\mathrm{ErRh}_4\mathrm{B}_4$ and $\mathrm{Ho}_x\mathrm{Mo}_6\mathrm{S}_8$ is quenched by onset of ferromagnetic order at a low temperature.[1,4-6] On the other hand, in $\mathrm{Dy}_x\mathrm{Mo}_6\mathrm{S}_8$ and $\mathrm{Er}_x\mathrm{Mo}_6\mathrm{S}_8$ superconductivity coexists with an antiferromagnetic order at low temperatures.[7,8] The upper critical field H_{c2} of $\mathrm{Er}_x\mathrm{Mo}_6\mathrm{S}_8$ and $\mathrm{Dy}_x\mathrm{Mo}_6\mathrm{S}_8$ has a maximum at a finite temperature above the magnetic-phase-transition point.[7]

The following model for the compounds is implied from the experimental facts.[2,9,10] Electrons responsible for superconductivity are the $4d$ electrons of Rh and Mo. The rare-earth ions carry magnetic moments, and the interaction between them mainly originates from the indirect coupling through the spin polarization of the $5d$ and $6s$ electrons of rare-earth ions. The spin-dependent interaction between superconducting electrons and rare-earth ions is extremely weak.

We believe that the effect mentioned below is most important for understanding the physical properties of the magnetic superconductors, especially of those with low-critical fields. In the compounds, the superconducting-phase-transition temperature is usually higher than the magnetic-phase-transition temperature. Let us consider the mixed state in the temperature region between the superconducting- and the magnetic-phase-transition temperatures. The persistent current of vortices induces a magnetic field. This magnetic field polarizes the spins of rare-earth ions[11] and produces a nonuniform spin magnetization with the periodicity of a flux-line lattice in the crystals. Since this spin-polarization effect becomes large near the magnetic Curie temperature, this nonuniformity may be observed by neutron scattering. Along with the vortex current, the spin magnetization contributes to the magnetic flux in the magnetic superconductors. The total flux of a single vortex which is the sum of spin and current contributions is quantized. Therefore, the flux quantization leads to the following situation: the vortex current is drastically affected by the spin magnetization and the current inversion occurs in some portion of the vortex. The current inversion causes the attractive force between the vortices. The magnetization curve is strongly influenced by the attractive interaction. As a result, the magnetic compounds have a tendency to become a type-I or type-II-1 superconductor even when they have a large κ. When temperature approaches the magnetic-phase-transition temperature, H_{c2} is drastically decreased. This fact explains the experimental results that H_{c2} has a maximum at a temperature above the magnetic-phase-transition temperature in $\mathrm{Dy}_x\mathrm{Mo}_6\mathrm{S}_8$ and $\mathrm{Er}_x\mathrm{Mo}_6\mathrm{S}_8$.[7]

When the spin-dependent interaction between conduction electrons and rare-earth ions exists, the fluc-

tuation of the rare-earth spins inside a Cooper pair acts as a pair breaker and weakens the BCS coupling constant.[12–14] Since the spin fluctuation is dependent on temperature and magnetic field, the BCS coupling constant becomes dependent on these quantities. In some of the magnetic superconductors, this effect should be taken into account. However, in the present paper, we neglect this effect and concentrate ourselves in discussions of the spin-magnetization effect mentioned above, assuming that the BCS coupling constant is independent of temperature and magnetic field. The effects of the spin splitting of conduction bands and the spin-orbit scattering are also neglected.

In Secs. II–IV the magnetic properties of rare-earth compounds will be presented. To prepare for a precise analysis of superconductivity, we need three relations which should be derived from the BCS theory. The first one is the Maxwell-type equation which determines the local magnetic field inside the metal. This equation is obtained when we determine the current as a function of the electromagnetic vector potential. An old example of an equation of this type is the Pippard equation. A usual way of calculating the current is to use the order parameter. The most well-known equation for the order parameter is the Gor'kov equation. Since the Gor'kov equation contains the internal electromagnetic vector potential, it should be coupled with the Pippard-type equation. Finally, we need the Gibbs free energy in order to relate the internal field to the external magnetic field. When the internal field and the external field are approximately equal, the Maxwell-type equation and the Gibbs free energy are unnecessary since we can then simply relate the external field to the order parameter through the Gor'kov equation. Such a situation occurs, for example, when one calculates H_{c2} with high-vortex density. The situation becomes more involved when the internal field is considerably different from the external field. In such a case, the internal field should be determined by the Maxwell-type equation and the Gibbs free energy determines only the vortex density. A main contribution of the boson theory[15–17] to the study of superconductivity has been the derivation of a precise form of the Maxwell-type equation *from the BCS theory.* Let us call this equation the new Pippard equation or the Maxwell-type equation.

In the boson theory all of the observables become functionals of the so-called boson-transformation parameter $f(x)$; the current $\vec{j}[f]$, the electromagnetic vector potential $\vec{a}[f]$, the order parameter $\Delta[f]$, etc. In this way, the quantities $\vec{j}$, $\vec{a}$, and Δ are related to each other through the function f. Calculating $j[\vec{f}]$ and feeding it into the Maxwell equation, we obtain the new Pippard equation. This is the Maxwell-type equation in the boson theory. Since this equation relates the vector potential $\vec{a}$ to the boson-transformation function f, $\vec{a}$ *and* Δ *are implicitly coupled to each other through this equation.* This is the reason why the current in the boson theory can be obtained directly from the Maxwell-type equation without any use of the equation for the order parameter. Presence of the function $f(x)$ makes this Maxwell-type equation quite different from the old Pippard equation. Another improvement in the derivation of the new Pippard equation lies in the calculation of the form factor (i.e., the c function) in front of the vector potential. This form factor originates from the *proper self-energy diagram.* It is well known that this self-energy has a pole singularity corresponding to a gapless energy (the so-called energy of the collective mode). Since the pole has a dominant effect on the form factor, particular care was taken in treatment of the electromagnetic effect in order to preserve the pole effect without violating gauge invariance. Such a gauge invariant treatment was not easy until the mechanism of spontaneous breakdown of the *gauge symmetry* in quantum field theory (i.e., the Higgs mechanism in terminology of high-energy physicists) was well understood. A part of the difficulty in understanding the Higgs mechanism was due to the lack of a simple and rigorous treatment of the gauge in quantum electrodynamics. This difficulty was solved by Nakanishi's formulation[18] of the gauge theory and the Higgs mechanism has been well understood in the past ten years. The gauge invariant calculation was helped also by a new technique in quantum field theory. In the past decade, there has been an extensive study of extended objects in quantum field theory. Among many studies along this line there has emerged a method for the analysis of extended objects (such as vortices, etc.) in quantum many-body systems. This method is based on the use of a certain operator transformation called the boson transformation. Appearance of the function f in the Maxwell-type equation is a result of this transformation.[16] The analysis of the Higgs mechanism disclosed the fact that the current in superconductors appears only in the vicinity of certain (topological) singularities such as the line singularity of a vortex or the surface singularities associated with boundary surfaces. These singularities appear through the function f and prohibit its Fourier transform. In the Maxwell-type equation, the role of the function $f(x)$ is to determine the kind of singularities under consideration and also to couple the vector potential to the order parameter. The appearance of $\vec{\nabla} \times \vec{\nabla} f(x)$ in the expression (2.11) for the energy clearly shows that only the topological singularities contribute to observable phenomena, because $\vec{\nabla} \times \vec{\nabla} f$ obviously vanishes unless f has a topological singularity. The equation for the function $f(x)$ depends on the choice of the gauge because $f(x)$ is the phase of the order parameter. However, as was pointed out above, only the singular part of $f(x)$

contributes to observable effects and this singular part satisfies the simple Laplace equation (2.6). The nonlocal factor [the c function in Eq. (2.5)] in the Maxwell-type equation is closely related to the Bethe-Salpeter amplitude of the collective mode[15] and also to the longitudinal plasma energy dispersion relation.[16,17] This function has been obtained[19] from the BCS Hamiltonian [the result is summarized in Eq. (3.12)]. Although the Maxwell-type equation has certain nonlinear terms, it can be shown[16] that such nonlinear terms are quite small. However, a considerable amount of nonlinear effect appears in the calculation of the vortex core energy. Up to now, the derivation of the new Pippard equation by the boson transformation method is more refined than the estimation of the core energy.[17] Although the derivation of the Maxwell-type equation is extremely involved, the tedious work is rewarded by the fact that, once the singularity in $f(x)$ is specified, the vortex current distribution and the internal magnetic field in the entire space can be obtained from the Maxwell-type equation.

The present paper is aimed at a study of magnetic superconductors, and not at the presentation of a detailed account of the derivation of the boson method, which can be found elsewhere.[16,17] However, we have made an analysis which shows how the approximations used in the boson method are related to those used in derivation of the Gor'kov equation and the Ginzburg-Landau (GL) equation. The result of this analysis will be published in a separate paper. Since all of the available theories use some kind of approximation, experiments should be the final judge of which method should be used under what condition. Nowadays, a large amount of very precise experimental data is available to us. For example, a highly precise experimental analysis of the first-order phase transition of Nb at $H = H_{c1}$ and also of its anisotropic behavior has been made by a narrow-angle neutron scattering experiment.[20,21] A relatively easy computation based on the Maxwell-type equation of the boson theory leads us to a precise description of the intervortex interaction and the results have been favorably compared with the above experimental data.[20,22] Another notable application[23] of the boson theory was the explanation of an anomaly observed by Fukase *et al.*[24] in their experiments on ultrasonic attenuation in a virgin single crystal of V_3Si. In this case the boson theory was useful because the external field is much weaker than H_{c2} (that is, the order parameter is not small and the internal field is very much different from the external field).

In this paper, we use the boson theory because our calculations involve the analysis of H_{c1} among others. Another reason for use of the boson theory is that it is an easy task to generalize the new Pippard equation to include the localized spin-magnetization effects.

In Sec. II, we reformulate the boson theory in a form applicable to the magnetic superconductors. In Sec. III, we calculate the magnetic field and induction of a single vortex and discuss how these quantities are influenced by the spin-magnetization effect. In Sec. IV, we obtain the temperature dependence of the upper and lower critical fields, and the magnetization curves.

II. ELECTROMAGNETIC FIELD EQUATIONS FOR MAGNETIC SUPERCONDUCTORS

The magnetic induction $\vec{b}$ is defined by a sum of the magnetic field $\vec{h}$ induced by the persistent current $\vec{j}$ and the spin magnetization $\vec{m}$ as

$$\vec{b} = \vec{h} + 4\pi \vec{m} \ . \tag{2.1}$$

The Maxwell equation is

$$\vec{\nabla} \times \vec{h} = \frac{4\pi}{c}\vec{j} + \frac{1}{c}\frac{\partial \vec{e}}{\partial t} \ , \tag{2.2}$$

$\vec{e}$ being the electric field. Introducing the vector potential $\vec{a}$, we express $\vec{b}$ and $\vec{e}$ as

$$\vec{b} = \vec{\nabla} \times \vec{a} \ , \tag{2.3}$$

$$\vec{e} = -\frac{1}{c}\frac{\partial \vec{a}}{\partial t} \ . \tag{2.4}$$

Since we are concerned with phenomena which change much slower than the plasma oscillation, $\vec{a}$ and $\vec{j}$ stand for their transverse components.[15–17] The current $\vec{j}$ in Eq. (2.2) is given by Eq. (8.24) in Ref. 15 as

$$\vec{j} = \frac{c^2 \hbar}{4\pi \lambda_L^2 e} \int d^3y \, c(\vec{x}-\vec{y}) \times \left(\vec{\nabla}_y f(\vec{y}) - \frac{e}{c\hbar}\vec{a}(\vec{y}) \right) \ , \tag{2.5}$$

where λ_L is the London penetration depth. The function $f(x,t)$ in Eq. (2.5) is equal to half the phase of the superconducting order parameter. This function has to be a solution of the Laplace equation

$$\nabla^2 f = 0 \ , \tag{2.6}$$

and satisfies correct boundary conditions.[15–17] In Eq. (2.5), $c(\vec{x})$ is the boson characteristic function[15–17] and its explicit form is given in Sec. III.

We restrict ourselves to the paramagnetic phase. Then, the spin magnetization $\vec{m}$ is connected with the magnetic field $\vec{h}$ by using the nonlocal susceptibility $\chi(\vec{x}-\vec{y})$ as

$$\vec{m}(\vec{x}) = \int d^3y \, \chi(\vec{x}-\vec{y})\,\vec{h}(\vec{y}) \ . \tag{2.7}$$

Taking the curl on both sides of Eq. (2.1) and using

Eqs. (2.2), (2.3), (2.4), and (2.7), we have

$$\vec{\nabla}\times\vec{b}(x)=\frac{c\hbar}{\lambda_L^2 e}\int d^3y\, c(x-y)\left[\vec{\nabla}_y f(\vec{y})-\frac{e}{c\hbar}\vec{a}(\vec{y})\right]$$
$$-\frac{1}{c^2}\frac{\partial^2}{\partial t^2}\vec{a}(x)$$
$$+4\pi\int d^3y\,\vec{\nabla}_x\times\left[\chi(\vec{x}-\vec{y})\vec{h}(\vec{y})\right] . \quad (2.8)$$

The Eqs. (2.1), (2.3), (2.7), and (2.8) construct a set of equations for determining $\vec{b}$, $\vec{h}$, $\vec{m}$, and $\vec{e}$ for a given $f(x,t)$.

The electronic energy of the system is given by Eq. (8.30) of Ref. 15 as

$$W=\frac{c\hbar}{2e}\int d^3x\left[\vec{\nabla}f(\vec{x})-\frac{e}{c\hbar}\vec{a}(\vec{x})\right]\cdot\vec{j}(\vec{x}) . \quad (2.9)$$

In a static case, Eq. (2.9) is rewritten by Eqs. (2.2) and (2.3) as

$$W=\frac{c\hbar}{8\pi e}\int d^3x\,[\vec{h}(\vec{x})\cdot\vec{\nabla}\times\vec{\nabla}f(\vec{x})]$$
$$-\frac{1}{8\pi}\int d^3x\,\vec{h}(x)\cdot\vec{b}(x) . \quad (2.10)$$

By adding the magnetostatic energy to W, the total energy of the system is obtained as

$$E=W+\frac{1}{8\pi}\int d^3x\,\vec{h}(\vec{x})\cdot\vec{b}(\vec{x})$$
$$=\frac{c\hbar}{8\pi e}\int d^3x\,[\vec{h}(\vec{x})\cdot\vec{\nabla}\times\vec{\nabla}f(\vec{x})] . \quad (2.11)$$

A more rigorous derivation of the energy expression (2.11) is given in the Appendix. There it will be shown also that Eq. (2.11) holds true even when anisotropic properties of superconductors are taken into account.

III. SINGLE VORTEX

Let us consider a vortex along the x_3 axis. We pay attention to the variation of physical quantities in the x_1 and x_2 plane, since they are independent of x_3. Hereafter, $\vec{x}$ means the two-dimensional vector, i.e., $\vec{x}=(x_1,x_2)$. The solution of Eq. (2.6) for a single vortex fulfills the equation[15–17]

$$\vec{\nabla}\times\vec{\nabla}f(\vec{x})=\pi\mu\vec{e}_3\delta(x) , \quad (3.1)$$

where $\vec{e}_3$ is the unit vector in the third direction and μ is an integer. Operating $\vec{\nabla}\times$ on both sides of Eq. (2.8), we have

$$\vec{\nabla}\times\left[\vec{\nabla}\times\vec{b}(\vec{x})\right]=\frac{c\hbar}{\lambda_L^2 e}\int d^2y\, c(\vec{x}-\vec{y})\left[\vec{\nabla}_y\times\vec{\nabla}_y f(\vec{y})-\frac{e}{c\hbar}\vec{b}(\vec{y})\right]+4\pi\int d^2y\,\vec{\nabla}_x\times\vec{\nabla}_x\times\left[\chi(\vec{x}-\vec{y})\vec{h}(\vec{y})\right] . \quad (3.2)$$

The quantities $\vec{h}$ and $\vec{b}$ are parallel to the third axis. The equation for the magnitudes of these quantities is obtained from Eqs. (3.1) and (3.2) as

$$\nabla^2 b(\vec{x})=-\frac{\mu\phi}{\lambda_L^2}c(\vec{x})+\frac{1}{\lambda_L^2}\int d^2y c(\vec{x}-\vec{y})b(\vec{y})$$
$$+4\pi\int d^2y h(\vec{y})\nabla_y^2\chi(\vec{x}-\vec{y}) , \quad (3.3)$$

where ϕ is the unit magnetic flux $hc/2e$. The Fourier transform of Eq. (3.3) is

$$k^2 b_k=\frac{\mu\phi}{\lambda_L^2}c_k-\frac{1}{\lambda_L^2}c_k b_k+4\pi k^2 h_k\chi_k , \quad (3.4)$$

where the Fourier transform of a function $g(x)$ is defined by

$$g(\vec{x})=\frac{1}{(2\pi)^2}\int d^2k\, g_k e^{i\vec{k}\cdot\vec{x}} . \quad (3.5)$$

The Fourier transform of Eq. (2.1) is

$$b_k=(1+4\pi\chi_k)h_k . \quad (3.6)$$

From Eqs. (3.4) and (3.6), h_k is calculated as

$$h_k=\mu\phi\frac{c_k}{\lambda_L^2 k^2+c_k(1+4\pi\chi_k)} . \quad (3.7)$$

We thus obtain the magnetic field

$$h(x)=\frac{\mu\phi}{(2\pi)^2}\int d^2k\,\frac{c_k}{\lambda_L^2 k^2+c_k(1+4\pi\chi_k)}e^{i\vec{k}\cdot\vec{x}} . \quad (3.8)$$

According to Eqs. (2.11) and (3.1), the self-energy of the vortex and the interaction energy between the vortices whose centers are at 0 and x are given, respectively, by

$$\mu\frac{\phi}{8\pi}h(0) , \quad (3.9)$$

and

$$\mu\frac{\phi}{8\pi}h(x) . \quad (3.10)$$

From Eqs. (3.6) and (3.7), b_k is obtained as

$$b_k=\mu\phi\frac{c_k(1+4\pi\chi_k)}{\lambda_L^2 k^2+c_k(1+4\pi\chi_k)} . \quad (3.11)$$

This expression of b_k shows that the total flux is quantized as

$$\int d^2x\, b(\vec{x}) = b_0 = \mu\phi \quad .$$

The form factor of the vortex for neutron scattering is proportional to b_k.

We study how $h(\vec{x})$ and b_k are affected from the presence of spin-magnetic moments in crystals. As was mentioned in the Introduction, we assume that the BCS coupling constant V is independent of temperature and magnetic field. Then, the Fourier amplitude of the boson characteristic function is well approximated for $0.2 \leq VN(0) \leq 0.4$, $N(0)$ being the density of states at the Fermi level, by[19]

$$c_k = \exp\{-\nu[\bar{k}/\kappa(t)]^\eta\} \quad , \tag{3.12}$$

$$\bar{k} = \lambda_L(t)k \quad , \tag{3.13}$$

$$\kappa(t) = [1/\gamma(t)][\lambda_L(t)/\lambda_L(0)]\kappa_B \quad , \tag{3.14}$$

$$\nu = -0.4257\, VN(0) + 0.559 \quad , \tag{3.15}$$

$$\eta = -0.7857\, VN(0) + 2.207 \quad , \tag{3.16}$$

where κ_B is $\lambda_L(0)/\xi_0$, ξ_0 being the coherence length at absolute zero, and t is the normalized temperature T/T_c. The function $\gamma(t)$ is given by

$$\gamma(t) = 1 + a\frac{t^n}{(1-t)^m} \quad , \tag{3.17}$$

$$a = -0.0536\, VN(0) + 0.3719 \quad , \tag{3.18}$$

$$n = 0.3714\, VN(0) + 3.846 \quad , \tag{3.19}$$

$$m = -0.0414\, VN(0) + 0.556 \quad . \tag{3.20}$$

The temperature dependence of the London penetration depth, $\lambda_L(t)/\lambda_L(0)$, is calculated from the relation

$$\left[\frac{\lambda_L(0)}{\lambda_L(t)}\right]^2 = 1 + 2\int d\epsilon \frac{\partial f_E}{\partial E} \quad , \tag{3.21}$$

where $f_E = [\exp(\beta E) + 1]^{-1}$ and $E = [\epsilon^2 + \Delta^2(t)]^{1/2}$, $\Delta(t)$ being the fermion gap. In the above expressions, the mean-free-path effect is not included explicitly. However, as was shown in Refs. 25 and 26, this effect can be taken into account by the scaling of κ. Therefore, the effect is considered to be included implicitly in the value of κ_B in Eq. (3.14).

In ferromagnets where the spin fluctuations with small wave numbers are dominant near the Curie temperature,[26] the staggered susceptibility χ_k is written

$$\chi_k = \frac{C}{T - T_m + Dk^2} = \frac{c/4\pi}{\epsilon + d\bar{k}^2} \quad , \tag{3.22}$$

$$c = \frac{4\pi C}{T_m} \quad , \tag{3.23}$$

$$d = D/T_m\lambda_L^2 \quad , \tag{3.24}$$

$$\epsilon = (T - T_m)/T_m \quad , \tag{3.25}$$

where C is the Curie constant, T_m is the Curie temperature, and D is the quantity proportional to the second derivative of the exchange interaction with respect to k. The normalized temperature t is related to ϵ by

$$t = (T_m/T_c)(1 + \epsilon) \quad . \tag{3.26}$$

In antiferromagnets, the spin fluctuations around $\vec{Q}$ are dominant near the Néel temperature, $\vec{Q}$ being the wave number which specifies the magnetic structure below the Néel temperature. The function c_k diminishes drastically for k above $1/\xi$, ξ being the coherence length. Since Q is much larger than $1/\xi$ in usual antiferromagnets, χ_k in the expressions of h_k and b_k is well approximated by χ_0

$$\chi_0 = \frac{C}{T - \Theta} = \frac{c/4\pi}{\epsilon + \epsilon_0} \quad , \tag{3.27}$$

$$\epsilon_0 = (T_m - \Theta)/T_m \quad , \tag{3.28}$$

where Θ is the paramagnetic Curie temperature and T_m is the Néel temperature in this case.

Next we show the result of numerical calculation for $h(r)$ and b_k. In the present paper, we use $VN(0) = 0.3$ and $t_m = T_m/T_c = 0.1$, and calculate $h(r)$ by means of Eq. (3.8). In ferromagnets, we choose two sets of parameters: $\kappa_B = 1$, $d = 0.1$, and $t = 0.4$ for Fig. 1(a), and $\kappa_B = 5$, $d = 0.1$, and $t = 0.2$ for Fig. 1(b). As the normalized Curie constant, we take the four values; $c = 0$, 1, 2, and 3. The value of $c = 0$ corresponds to the nonmagnetic superconductor. The value of c is estimated to be 2.58 for $ErRh_4B_4$ and 1.73 for $Ho_{1.2}Mo_6S_8$. As is seen from Fig. 1, $h(r)$ decreases as c increases. The negative part of $h(r)$, which is the attractive interaction of the intervortex force, appears at its tail. When c increases, the position of the minimum of $h(r)$ shifts toward the center of vortex and its depth increases. We show $h(r)$ for antiferromagnets in Fig. 2(a) and 2(b). The parameters are $\kappa_B = 1$, $\epsilon_0 = 1$, and $t = 0.4$ for Fig. 2(a), and $\kappa_B = 5$, $\epsilon_0 = 1$, and $t = 0.2$ for Fig. 2(b). As is seen in these figures, $h(r)$ of antiferromagnets has a similar tendency as that of ferromagnets, but the rate of decrease of $h(r)$ with increasing c is weaker than that of ferromagnets.

We calculate b_k by using Eq. (3.11), and show the results for ferromagnets in Fig. 3 and for antiferromagnets in Fig. 4. The value of b_k at $k = 0$ is unity, indicating the flux quantization. The decrease of b_k with increasing k becomes slower for large values of c. This tendency is prominent when the temperature approaches the magnetic-phase-transition temperature. This behavior is expected to be observed by small angle scattering of neutrons.

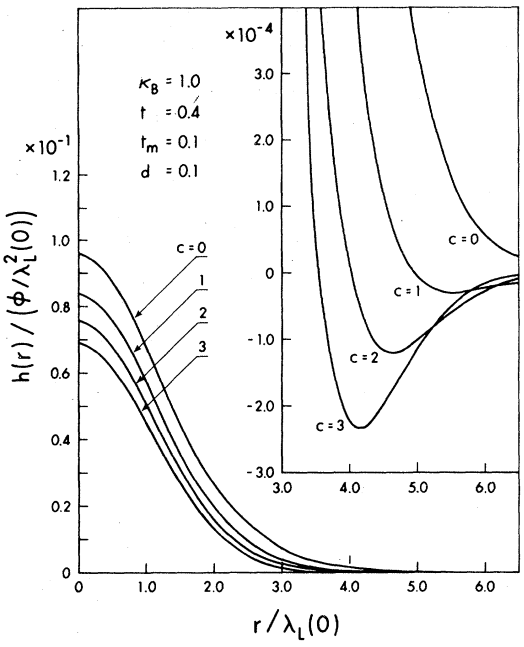

(a)

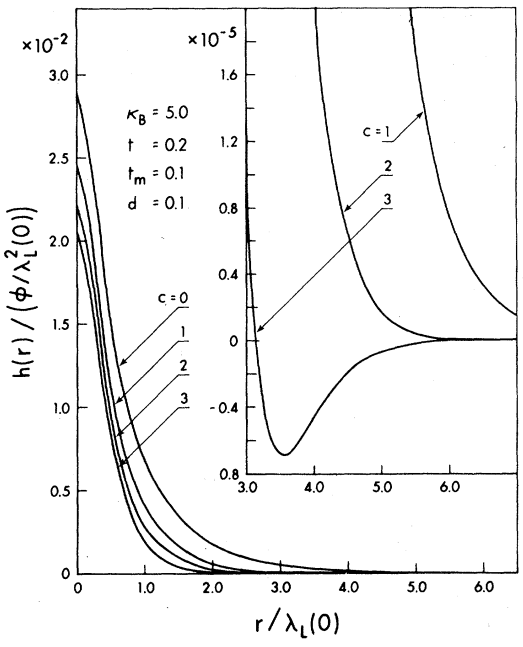

(b)

FIG. 1. (a) Magnetic field distribution of a single vortex in a ferromagnetic superconductor with $\kappa_B = 1$. The one for a nonmagnetic superconductor ($c = 0$) is also plotted. (b) Magnetic field distribution of a single vortex in a ferromagnetic superconductor with $\kappa_B = 5$. The one for a nonmagnetic superconductor ($c = 0$) is also plotted.

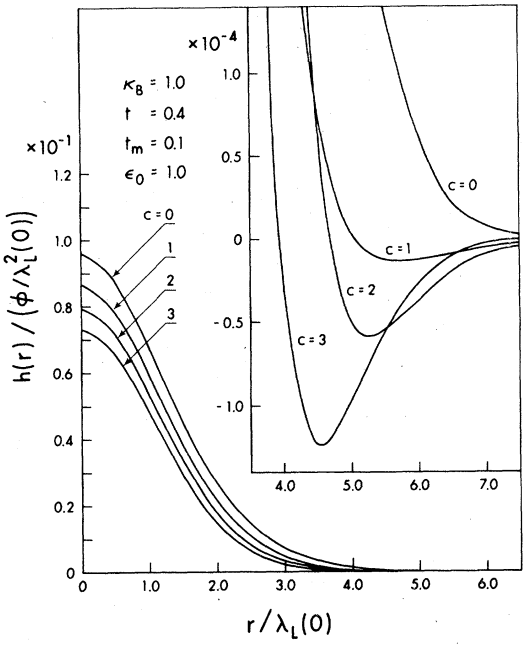

(a)

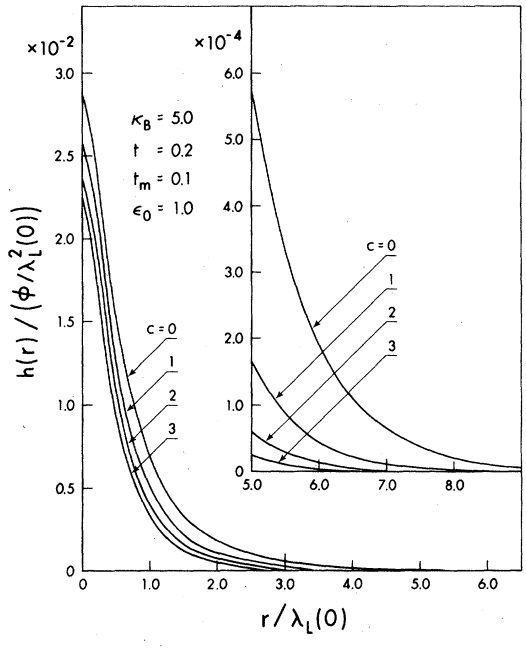

(b)

FIG. 2. (a) Magnetic field distribution of a single vortex in an antiferromagnetic superconductor with $\kappa_B = 1$. The one for a nonmagnetic superconductor ($c = 0$) is also plotted. (b) Magnetic field distribution of a single vortex in an antiferromagnetic superconductor with $\kappa_B = 5$. The one for a nonmagnetic superconductor ($c = 0$) is also plotted.

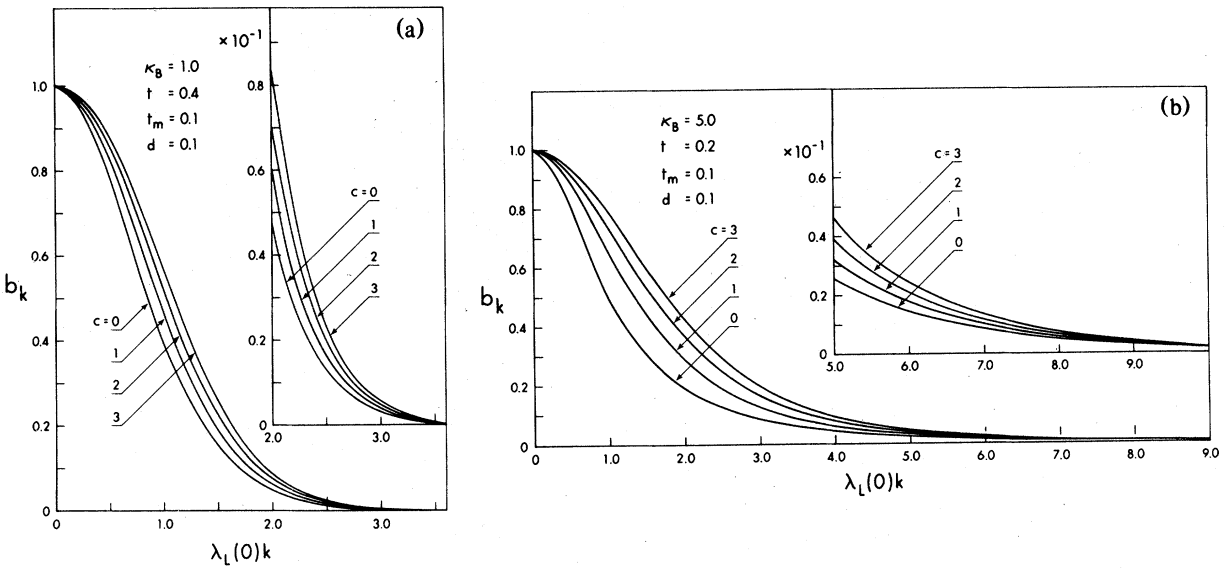

FIG. 3.(a) Wave-number dependence of the Fourier amplitude of the magnetic induction of a single vortex (the single-vortex neutron scattering form factor) in a ferromagnetic superconductor with $\kappa_B = 1$. The one for a nonmagnetic superconductor ($c = 0$) is also plotted. (b) Wave-number dependence of the Fourier amplitude of the magnetic induction of a single vortex (the single-vortex neutron scattering form factor) in a ferromagnetic superconductor with $\kappa_B = 5$. The one for a nonmagnetic superconductor ($c = 0$) is also plotted.

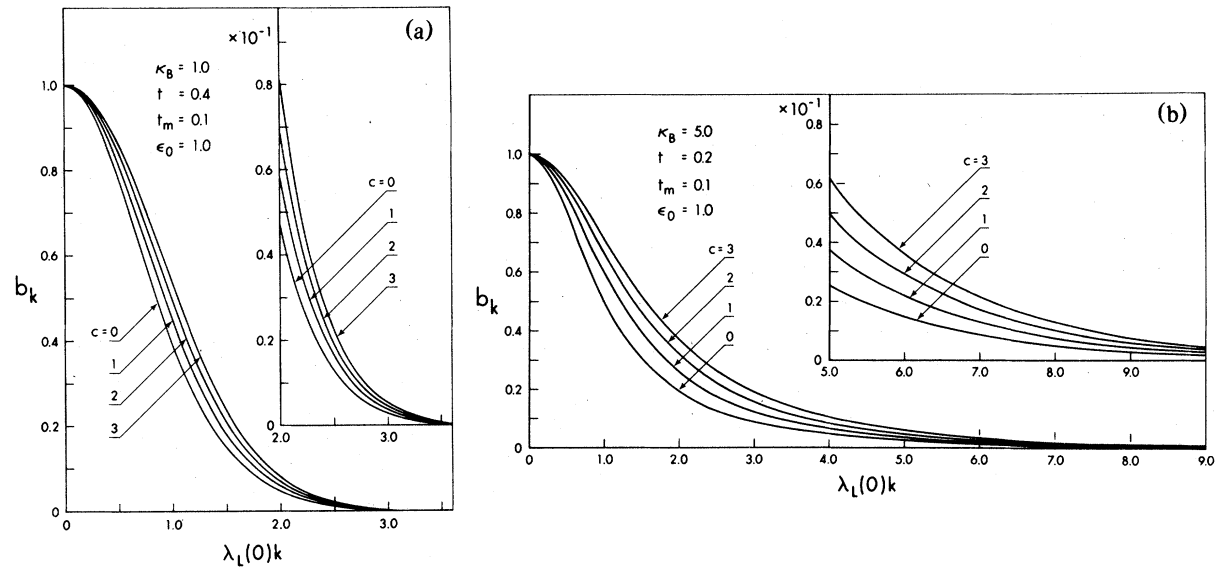

FIG. 4.(a) Wave-number dependence of the Fourier amplitude of the magnetic induction of a single vortex (the single-vortex neutron scattering form factor) in an antiferromagnetic superconductor with $\kappa_B = 1$. The one for a nonmagnetic superconductor ($c = 0$) is also plotted. (b) Wave-number dependence of the Fourier amplitude of the magnetic induction of a single vortex (the single-vortex neutron scattering form factor) in an antiferromagnetic superconductor with $\kappa_B = 5$. The one for a nonmagnetic superconductor ($c = 0$) is also plotted.

IV. MAGNETIZATION, AND UPPER AND LOWER CRITICAL FIELDS

The energy density of the vortices is given from Eqs. (3.9) and (3.10) by

$$W=\frac{n\mu\phi}{8\pi}\sum_i h(\zeta_i) \ , \tag{4.1}$$

where $\zeta_i (i=1,2,\dots)$ denotes the position of the vortex center and n is the vortex density. As discussed in Refs. 17 and 27 for obtaining the total energy density of the vortices, we should add the normal core energy density to the energy density (4.1). The normal core energy density is written

$$W_n=n\left[E_1-E_2\sum_{i\neq 0} h(\zeta_i)\right] \ , \tag{4.2}$$

where E_1 is the normal core energy per unit length for an isolated vortex and given by

$$E_1=\hbar^2c^2/32e^2\lambda_L^2(t) \ . \tag{4.3}$$

The second term in the parentheses of Eq. (4.2) expresses a correction term which comes from the interaction among the vortex cores. The value of the parameter E_2 is determined by thermodynamical conditions. The Gibbs free energies of the mixed state and the normal state, G_s and G_n, are respectively given by

$$G_s=\frac{n\mu\phi}{8\pi}\sum_i h(\zeta_i)+n\left[E_1-E_2\sum_{i\neq 0} h(\zeta_i)\right]-\frac{HB}{4\pi} \tag{4.4}$$

and

$$G_n=\frac{H_c^2}{8\pi}-\frac{HB}{8\pi} \ , \tag{4.5}$$

where H and B are the thermodynamical magnetic field and induction, respectively, and H_c is the thermodynamical critical field. The condition $\partial G_s/\partial n=0$ gives H as a function of n,

$$H=\frac{1}{2}\frac{\partial}{\partial n}n\sum_i h(\zeta_i)+\frac{4\pi}{\mu\phi}E_1 -\frac{4\pi}{\mu\phi}E_2\frac{\partial}{\partial n}n\sum_{i\neq 0} h(\zeta_i) \ . \tag{4.6}$$

We determine E_2 from the condition that at the upper critical field H_{c2}, the Gibbs free energy and the magnetic induction of the mixed state are, respectively, equal to those of the normal state,

$$G_s=G_n \ , \tag{4.7}$$

$$B_s=B_n, \quad \text{or} \quad \mu n\phi=(1+4\pi\chi_0)H \ . \tag{4.8}$$

Equations (4.7) and (4.8) determine the critical value of n at H_{c2} (i.e., n_c) and E_2 simultaneously. The upper critical field is calculated by

$$H_{c2}=\mu\phi n_c/(1+4\pi\chi_0) \ . \tag{4.9}$$

The magnetization is obtained as a function of the magnetic field H from Eq. (4.6) and

$$4\pi M=\mu\phi n-H \ . \tag{4.10}$$

The free energy for $\mu=1$ is usually lower than those for higher values of μ. Therefore, we assume $\mu=1$ in the present paper. However, the case $\mu>1$ might not be excluded, because the free energies for higher values of μ are very close to that for $\mu=1$ in low temperature and high magnetic field, especially in magnetic superconductors. We assume that vortices form a triangle lattice with lattice constant d. The vortex density n is then given by $(2/\sqrt{3})(1/d^2)$. The reciprocal lattice is expressed by

$$k=2\pi nd(l^2+m^2-lm)^{1/2} \ , \tag{4.11}$$

l and m being integers. The sums $\sum_i h(\zeta_i)$ and $\sum_{i\neq 0} h(\zeta_i)$ appearing in Eqs. (4.4) and (4.6) are transformed into the sums in this reciprocal-lattice space as

$$\sum_i h(\zeta_i)=\sum_k h_k \ , \tag{4.12}$$

$$\sum_{i\neq 0} h(\zeta_i)=\sum_k h_k-\frac{1}{(2\pi)^2}\int d^2k\, h_k \ , \tag{4.13}$$

where h_k was given by Eq. (3.7).

Using Eqs. (3.22), (4.6), and (4.10), we numerically calculated the magnetization in ferromagnets as a function of external magnetic field H. In Fig. 5(a), $4\pi(M_n-M_s)$ is plotted as a function of H when the parameters $\kappa_B=1$, $t_m=0.1$, $d=0.1$, and $t=0.4$ are chosen. Here M_n and M_s are the magnetization of the normal and mixed state, respectively. The magnetic field at the peak head of the curve for $4\pi(M_n-M_s)$ corresponds to the lower critical field H_{c1}. The gradient of the magnetization curves below H_{c1} increases as c increases, because of an increase of the paramagnetic susceptibility in the normal state. The areas below all the magnetization curves should be the same. As is seen in the figure, the magnetization curves are of the type-II-1 superconductor, and the drop of magnetization at H_{c1} drastically increases as c increases. This increase is due to the shift of the position of minimum $h(r)$ toward the center of vortex, as is seen in Fig. 1(a). Figure 5(b) shows $4\pi(M_n-M_s)$ for $\kappa_B=5$, $t_m=0.1$, $d=0.1$, and $t=0.2$. In this case, all the magnetization curves are of the type-II-2 superconductor, but the magnetization decreases so fast at $H\gtrsim H_{c1}$ that it looks like the one for the type-II-1 superconductor. Figure 6 shows the magnetization curves for antiferromagnets.

Figure 7 shows the temperature dependence of the upper and lower critical fields. The value of H_{c2}

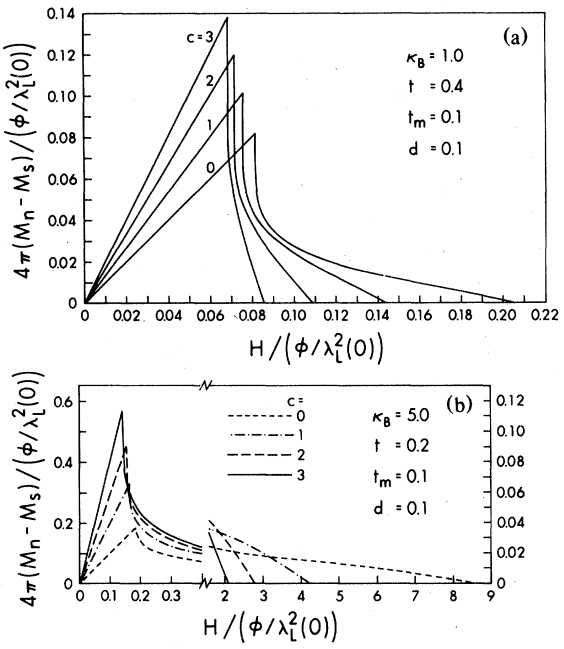

FIG. 5.(a) Magnetic field dependence of $4\pi(M_n - M_s)$ of a ferromagnetic superconductor with $\kappa_B = 1$, where M_n and M_s are the magnetizations of the normal and mixed state, respectively. The one for a nonmagnetic superconductor ($c = 0$) is also plotted. (b) Magnetic field dependence of $4\pi(M_n - M_s)$ of a ferromagnetic superconductor with $\kappa_B = 5$, where M_n and M_s are the magnetizations of the normal and mixed state, respectively. The one for a nonmagnetic superconductor ($c = 0$) is also plotted.

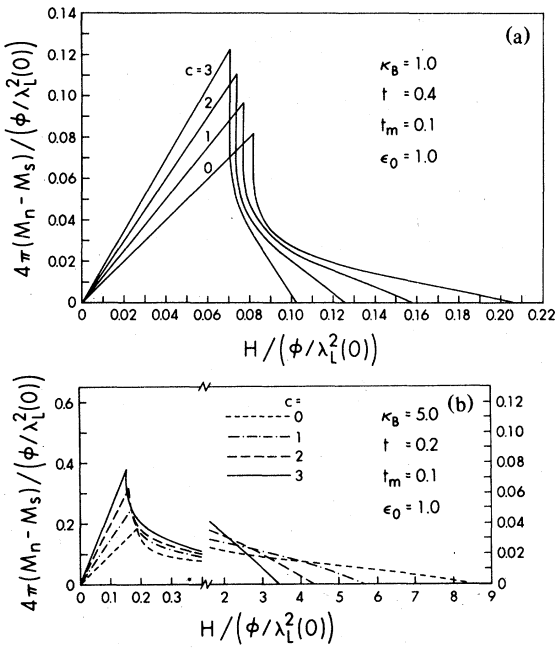

FIG. 6.(a) Magnetic field dependence of $4\pi(M_n - M_s)$ of an antiferromagnetic superconductor with $\kappa_B = 1$, where M_n and M_s are the magnetizations of the normal and mixed state, respectively. The one for a nonmagnetic superconductor ($c = 0$) is also plotted. (b) Magnetic field dependence of $4\pi(M_n - M_s)$ of an antiferromagnetic superconductor with $\kappa_B = 5$, where M_n and M_s are the magnetizations of the normal and mixed state, respectively. The one for a nonmagnetic superconductor ($c = 0$) is also plotted.

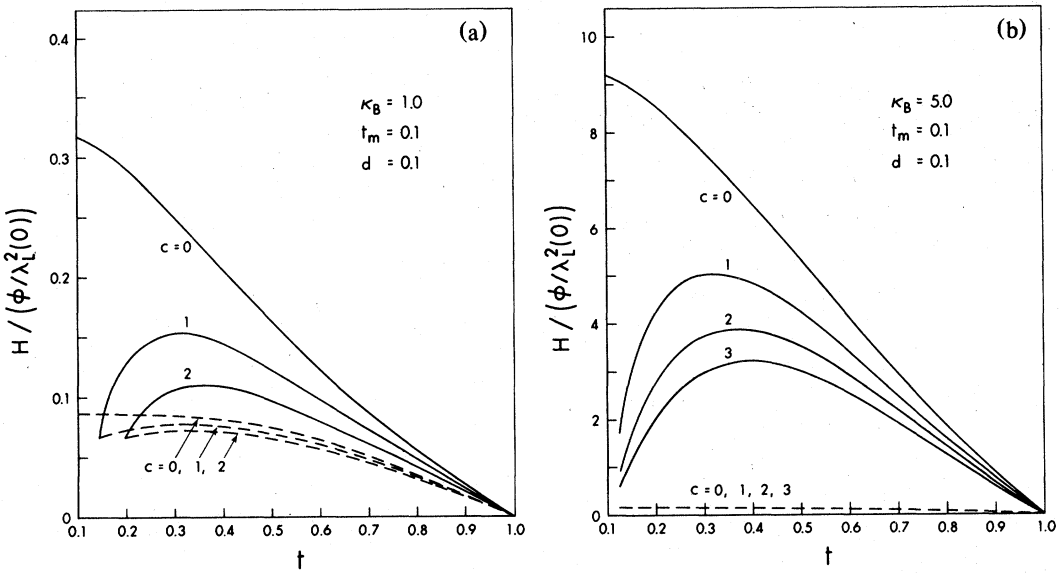

FIG. 7.(a) Temperature dependence of the critical fields in a ferromagnetic superconductor with $\kappa_B = 1$. The solid and dashed lines represent H_{c2} and H_{c1}, respectively. The one for a nonmagnetic superconductor ($c = 0$) is also plotted. Below the temperature at which the solid and dashed curves coincide with each other, the crystal becomes the type-I superconductor. (b) Temperature dependence of the critical fields in a ferromagnetic superconductor with $\kappa_B = 5$. The solid and dashed lines represent H_{c2} and H_{c1}, respectively. The one for a nonmagnetic superconductor ($c = 0$) is also plotted.

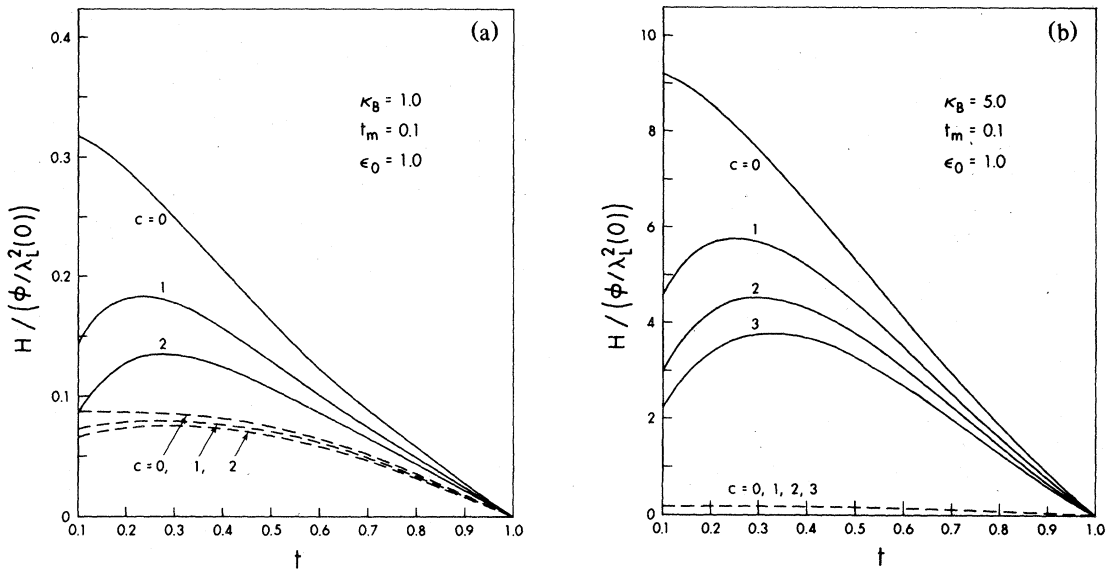

FIG. 8.(a) Temperature dependence of the critical fields in an antiferromagnetic superconductor with $\kappa_B = 1$. The solid and dashed lines represent H_{c2} and H_{c1}, respectively. The one for a nonmagnetic superconductor ($c = 0$) is also plotted. (b) Temperature dependence of the critical field in an antiferromagnetic superconductor with $\kappa_B = 5$. The solid and dashed lines represent H_{c2} and H_{c1}, respectively. The one for a nonmagnetic superconductor ($c = 0$) is also plotted.

is calculated by use of Eq. (4.9). The curves of H_{c2} indicated by the solid lines are strongly depressed near the magnetic-phase-transition temperature $t_m = 0.1$. The dashed curves show H_{c1}. Note that depression of H_{c1} due to the spin magnetization is much weaker than that of H_{c2}. Below the temperature at which the solid and dashed curves coincide with each other, the crystal makes a phase transition to the type-I superconducting state. Figure 7(b) shows the critical fields for $\kappa_B = 5$, $t_m = 0.1$, and $d = 0.1$. As seen in Fig. 7, the curves of H_{c2} have a maximum above t_m. This prediction seems to be consistent with the experimental results in $ErRh_4B_4$ by Fertig *et al.*[1] and in $Ho_xMo_6S_6$ by Ishikawa and Fischer.[5] The critical fields in antiferromagnets are shown in Fig. 8. In antiferromagnetic case too, H_{c2} has a maximum at a temperature above t_m. This behavior of H_{c2} has been observed in $Er_xMo_6S_8$ and $Dy_xMo_6S_8$ by Ishikawa and Fischer.[7]

ACKNOWLEDGMENTS

One of the authors (M.T.) expresses his sincere thanks to another author (H.U.) and the Theoretical Physics Institute of the University of Alberta for inviting him to the Institute, at which part of the present work was done. We would like to thank Dr. S. Maekawa and Mr. T. Koyama for valuable discussions, Mr. R. Teshima for his fine computational work, and Mr. S. Takahashi for the estimation of the values of c for $ErRh_4B_4$ and $Ho_{1.2}Mo_6S_8$. This work was supported by the Natural Science and Engineering Research Council, Canada and by the Faculty of Science of the University of Alberta.

APPENDIX: DERIVATION OF THE FORMULA (2.11) FOR VORTEX ENERGY

Since we are planning to extend our study of magnetic superconductors to take into account the anisotropic effects in our forthcoming paper, we consider here the anisotropic superconductors. A rigorous formulation of the boson theory for anisotropic superconductors was presented in Ref. 17. In static cases the macroscopic equation for $\vec{a}$ and f [cf., Eqs. (3.5) and (3.13) in Ref. 17] are

$$(\nabla^2\delta_{ij} - \nabla_i\nabla_j)a_j(\vec{x}) = \frac{1}{\lambda_L^2}\int d^3y\, c(\vec{x}-\vec{y})\,V_{ij}(\vec{\nabla}) \times \left[a_j(\vec{y}) - \frac{\hbar c}{e}\nabla_j f(\vec{y})\right] + L_{il}^T \delta m_{ij}^2(\vec{\nabla})a_j(\vec{x}) \,, \tag{A1}$$

$$V_{ij}(\vec{\nabla})\nabla_i\nabla_j f(\vec{x}) = 0 \,, \tag{A2}$$

where $\vec{\nabla}$ is the space derivative and L_{ij}^T is the projec-

tion operator of the transverse component

$$L_{ij}^T = \delta_{ij} - \nabla_i \frac{1}{\nabla^2} \nabla_j \ , \tag{A3}$$

which satisfies

$$L_{il}^T L_{lj}^T = L_{ij}^T \ . \tag{A4}$$

The derivative operators, $V_{ij}(\vec{\nabla})$ and $\delta m_{ij}^2(\vec{\nabla})$, in above relations are closely related to the plasma equation which determines the plasma energy. This can be seen from the free-field equation for plasma field U_μ^0 $(\mu = 0, 1, 2, 3)$,

$$\Lambda_{\mu\nu}(\partial) U_\nu^0 = 0 \ . \tag{A5}$$

The expression of $\Lambda_{\mu\nu}(\partial)$ was given by Eq. (3.8) in Ref. 17. In the following consideration we need only the spatial components of $\Lambda_{\mu\nu}(\partial)$:

$$\Lambda_{ij}(\partial) = \partial^2 \delta_{ij} - \nabla_i \nabla_j - m^2(\vec{\nabla}) V_{ij}(\vec{\nabla}) - L_{il}^T \delta m_{lj}^2(\vec{\nabla}) \ . \tag{A6}$$

Since λ_L and $c(\vec{k})$, which is the Fourier amplitude of $c(\vec{x})$, are defined by

$$\lambda_L = \frac{1}{m(0)} \ , \tag{A7}$$

$$c(\vec{k}) = \frac{m^2(i\vec{k})}{m^2(0)} \ , \tag{A8}$$

respectively, the macroscopic equation (A1) reads

$$\Lambda_{ij}(\partial) a_j(\vec{x}) = -m^2(\vec{\nabla}) V_{ij}(\vec{\nabla}) \frac{\hbar c}{e} \nabla_j f(x) \ . \tag{A9}$$

According to Eq. (3.6) in Ref. 17, we have the relation

$$L_{il}^T \delta m_{lj}^2(\vec{\nabla}) = \delta m_{il}^2(\vec{\nabla}) L_{lj}^T \ . \tag{A10}$$

Therefore, using Eq. (A4), we find

$$L_{il}^T \delta m_{lj}^2(\vec{\nabla}) a_j(\vec{x}) = L_{il}^T \delta m_{lk}^2(\vec{\nabla}) L_{kj}^T a_j(\vec{x}) \tag{A11}$$

$$= -[\vec{\nabla} \times \alpha(\vec{\nabla} \times \vec{a})]_i \tag{A12}$$

where α is a 3×3 matrix, whose elements $\alpha_{ij}(\vec{\nabla})$ are determined by the structure of δm_{ij}^2,

$$[\alpha(\vec{\nabla} \times \vec{a})]_i = \alpha_{ij}(\vec{\nabla})(\vec{\nabla} \times \vec{a})_j \ . \tag{A13}$$

Since δm_{ij}^2 is proportional to ∇^2 [cf., Eq. (3.10) in Ref. 17], we see that $\alpha_{ij}(0)$ does not diverge.

Now Eq. (A1) can be put in the form

$$[\vec{\nabla} \times \vec{b}(\vec{x})]_i = \frac{c\hbar}{\lambda_L^2 e} \int d^3y \, c(\vec{x} - \vec{y}) V_{ij}(\vec{\nabla}) \times \left[\nabla_j f(\vec{y}) - \frac{e}{c\hbar} a_j(\vec{y}) \right] + (\vec{\nabla} \times \alpha \vec{b})_i \ , \tag{A14}$$

where $\vec{b} = \vec{\nabla} \times \vec{a}$.

As it was shown in Ref. 17, in derivation of above macroscopic equation, use was made of the boson transformation[28] [cf., Eq. (2.53) in Ref. 17],

$$U_\mu^0(x) \to U_\mu^0(x) + a_\mu(x) \ , \tag{A15}$$

$$\chi^0(x) \to \chi^0(x) + \left(\frac{\hbar c}{e} \right) m(\vec{\nabla}) \left(\frac{v(\vec{\nabla})}{c} \right)^{-1} f(x) \ . \tag{A16}$$

Here χ^0 is the Goldstone boson, the energy of which is given by $\omega(i\vec{p})$ satisfying the relation of the form [cf., Eq. (3.1) in Ref. 17],[29]

$$\omega^2(i\vec{p}) = [v(i\vec{p})/c]^2 V_{ij}(i\vec{p}) p_i p_j \ . \tag{A17}$$

The derivative operator $v(\vec{\nabla})$ in Eq. (A16) is defined by this relation.

Since the energy of the static system is equal to the Lagrangian with minus sign, the energy created by the transformation (A15) is given by

$$W[a] = -\frac{1}{8\pi} \int d^3x \, a_i(\vec{x}) \Lambda_{ij}(\partial) a_j(\vec{x}) \ . \tag{A18}$$

The Hamiltonian of the Goldstone boson χ^0 has the form

$$H_0[\chi] = \frac{1}{8\pi} \int d^3x \, [(\chi^0)^2 + \chi^0 \omega(\vec{\nabla}) \chi^0] \ . \tag{A19}$$

The boson transformation (A16) applied to this Hamiltonian creates the following energy:

$$W[f] = \frac{1}{8\pi\lambda_L^2} \left(\frac{\hbar c}{e} \right)^2 \int d^3x \int d^3y \, \nabla_i f(\vec{x}) c(\vec{x} - \vec{y}) \times V_{ij} \nabla_j f(\vec{y}) \ . \tag{A20}$$

It was shown in Ref. 17 also that the boson transformation requires an adjustment of the gauge condition, which creates the following energy:

$$W_G[f] = -\frac{1}{4\pi\lambda_L^2} \left(\frac{\hbar c}{e} \right) \int d^3x \int d^3y \, a_i(\vec{x}) c(\vec{x} - \vec{y}) \times V_{ij} \nabla_j f(\vec{y}) \ . \tag{A21}$$

The total energy created by the boson transformation is

$$E = W[a] + W[f] + W_G[f] \ . \tag{A22}$$

Using Eq. (A9), we find that

$$W_G[f] = -2 W[a] \ , \tag{A23}$$

which leads to

$$E = W[f] + \tfrac{1}{2} W_G[f] \tag{A24}$$

$$= -\frac{1}{8\pi\lambda_L^2} \left(\frac{\hbar c}{e} \right) \int d^3x \int d^3y \left[a_i(\vec{x}) - \frac{\hbar c}{e} \nabla_i f(\vec{x}) \right] \times c(\vec{x} - \vec{y}) V_{jl} \nabla_j f(\vec{y}) \ . \tag{A25}$$

Now Eq. (A14) leads to

$$E=\frac{1}{8\pi}\left(\frac{\hbar c}{e}\right)\int d^3x\,[\vec{\nabla}\times(I-\alpha)\vec{b}(\vec{x})]\cdot\vec{\nabla}f(\vec{x})\ , \tag{A26}$$

where I is the 3×3 unit matrix,

$$[(I-\alpha)\vec{b}]_i=(\delta_{ij}-\alpha_{ij})b_j\ . \tag{A27}$$

We finally have

$$E=\frac{1}{8\pi}\left(\frac{\hbar c}{e}\right)\int d^3x\,(I-\alpha)\vec{b}(\vec{x})\cdot\vec{\nabla}\times\vec{\nabla}f(\vec{x})\ . \tag{A28}$$

In the case of the magnetic superconductors, the last term in the right-hand side of the macroscopic equation (A14) is the current due to the spin magnetization

$$\vec{\nabla}\times\alpha\vec{b}=4\pi\vec{\nabla}\times\vec{m}\ . \tag{A29}$$

Since $m_i=\chi_{ij}(\vec{\nabla})h_j$, we obtain from Eq. (A29) the relation

$$\alpha_{ij}(\vec{\nabla})b_j=4\pi\chi_{ij}(\vec{\nabla})h_j\ . \tag{A30}$$

Here $\chi(i\vec{p})=(\chi_{ij}(i\vec{p}))$ is the staggered susceptibility. Considering $\vec{b}=(1+4\pi\chi)\vec{h}$, we obtain

$$\alpha=\frac{4\pi\chi}{I+4\pi\chi}\ , \tag{A31}$$

which leads to

$$(I-\alpha)\vec{b}=\vec{h}\ . \tag{A32}$$

We thus find that the energy E is given by

$$E=\frac{\hbar c}{8\pi e}\int d^3x\,\vec{h}(x)\cdot\vec{\nabla}\times\vec{\nabla}f(x)\ . \tag{A33}$$

Equation (2.11) is now obtained.

The above argument shows that Eq. (2.11) holds true even when we take into account the anisotropy effect. Using Eq. (A31), we can rewrite the macroscopic equation (A14) as

$$[\vec{\nabla}\times\vec{b}(\vec{x})]_i=\frac{c\hbar}{\lambda_L^2 e}\int d^3y\,c(\vec{x}-\vec{y})V_{ij}(\vec{\nabla})\times\left[\nabla_j f(\vec{y})-\frac{e}{c\hbar}a_j(\vec{y})\right]+4\pi(\vec{\nabla}\times\chi\vec{h})_i\ . \tag{A34}$$

When we ignore the anisotropic effect, we have $V_{ij}=\delta_{ij}$. In this case Eq. (A34) becomes the macroscopic equation (2.8).

[1]W. A. Fertig, D. C. Johnston, L. E. Delong, R. W. McCallum, M. B. Maple, and B. T. Matthias, Phys. Rev. Lett. 38, 987 (1977).

[2]Ø. Fischer, A. Treyvaud, R. Chevrel, and M. Sergent, Solid State Commun. 17, 21 (1975).

[3]R. N. Shelton, R. W. McCallum, and H. Adrian, Phys. Lett. A 56, 213 (1976).

[4]D. E. Moncton, D. B. McWhan, J. Eckert, G. Shirane, and W. Thomlinson, Phys. Rev. Lett. 39, 1164 (1977).

[5]M. Ishikawa and Ø. Fischer, Solid State Commun. 23, 37 (1977).

[6]J. W. Lynn, D. E. Moncton, W. Thomlinson, G. Shirane, and R. N. Shelton, Solid State Commun. 26, 493 (1978).

[7]M. Ishikawa and Ø. Fischer, Solid State Commun. 24, 747 (1977).

[8]D. E. Moncton, G. Shirane, W. Thomlinson, M. Ishikawa, and Ø. Fischer, Phys. Rev. Lett. 41, 1133 (1978).

[9]Ø. Fischer, in *Proceedings of the Fourteenth International Conference on Low Temperature Physics Otaniemi, Finland, 1975,* edited by M. Krusius and M. Vuorio (North-Holland, Amsterdam, 1975), Vol. V, p. 14.

[10]Ø. Fischer, M. Decroux, R. Chevrel, and M. Sergent, in *Proceedings of the Second Rochester Conference Superconductivity in d- and f-Band Metals, University of Rochester, 1976,* edited by D. H. Douglass (Plenum, New York, 1976), p. 175.

[11]In the present paper, the spin of rare-earth ion stands for the total angular momentum consisting of the spin and orbital angular momenta of rare-earth ion.

[12]S. Maekawa and M. Tachiki, Phys. Rev. B 18, 4688 (1978).

[13]D. Rainer, Z. Phys. 252, 174 (1972).

[14]A. Sakurai, Solid State Commun. 25, 867 (1978).

[15]L. Leplae, F. Mancini, and H. Umezawa, Phys. Rev. C 10, 151 (1974).

[16]H. Matsumoto and H. Umezawa, Fortschr. Phys. 24, 357 (1976).

[17]H. Matsumoto, M. Tachiki, and H. Umezawa, Fortschr. Phys. 25, 273 (1977).

[18]N. Nakanishi, Prog. Theor. Phys. 49, 640 (1973); *ibid.* 50, 1388 (1973).

[19]I. Shapira, M. N. Shah, and H. Umezawa, Phys. Status Solidi B 84, 213 (1976).

[20]D. K. Christen, Proceedings of the Fourth International Conference on Small Angle Scattering of X-rays and Neutrons, October 1977, Gatlinburg, Tennessee (unpublished).

[21]D. K. Christen, S. Spooner, P. Thorel, and H. R. Kerchner, J. Appl. Crystal. 11, 650 (1978); *ibid.* 11, 654 (1978). D. K. Christen and P. Thorel, Phys. Rev. Lett. 42, 191 (1979).

[22]T. Koyama, M. Tachiki, H. Matsumoto, and H. Umezawa, Phys. Rev. B 20, 918 (1979).

[23]M. Tachiki and T. Koyama, Phys. Rev. B 15, 3339 (1977). M. Tachiki and H. Umezawa, Phys. Rev. B 15, 3332 (1977).

[24]T. Fukase, M. Tachiki, N. Toyota, and Y. Muto, Solid

State Commun. 18, 505 (1976); K. Akutsu, K. Noto, T. Fukase, N. Toyota, and Y. Muto, J. Phys. Soc. Jpn. 41, 1431 (1976).
[25]F. Mancini, M. Marinaro, and M. Zannetti, Phys. Status Solidi B 93, 291 (1978).
[26]S. De Lillo, F. Mancini, and H. Umezawa, Phys. Status Solidi B 95, 53 (1978).
[27]M. Tachiki and S. Maekawa, Prog. Theor. Phys. 51, 1 (1974).
[28]F. Mancini, M. Tachiki, and H. Umezawa, Phys. Status Solidi B 94, 1 (1978).
[29]As Eq. (2.53a) in Ref. 17 shows, there appears a renormalization factor Z_l in the transformation (A17). In this paper we approximately put $Z_l = 1$. When we do not use this approximation, $\vec{h}$ in Eq. (A34) is replaced by $Z_l^{-1}\vec{h}$.